J. Biochem. 130, 89–98 (2001)

Substrate Recognition Mechanism of Thermophilic Dual-Substrate Enzyme[1]

Hideaki Ura,[*] Tadashi Nakai,[†] Shin-ichi Kawaguchi,[*] Ikuko Miyahara,[†] Ken Hirotsu,[†] and Seiki Kuramitsu[*,‡,§,2]

[*]*Department of Biology, Graduate School of Science, Osaka University, 1-1 Machikaneyama-cho, Toyonaka, Osaka 560-0043;* [†]*Department of Chemistry, Graduate School of Science, Osaka City University, Sugimoto, Sumiyoshi-ku, Osaka 558-8585;* [‡]*Genomic Sciences Center, RIKEN Yokohama Institute, 1-7-22 Suehiro-cho, Tsurumi, Yokohama 230-0045; and* [§]*Harima Institute/SPring-8, 1-1-1 Koto Mikazuki-cho, Sayo-gun, Hyogo 679-5148*

Received March 5, 2001; accepted April 17, 2001

Aspartate aminotransferase from an extremely thermophilic bacterium, *Thermus thermophilus* HB8 (ttAspAT), has been believed to be specific for an acidic substrate. However, stepwise introduction of mutations in the active-site residues finally changed its substrate specificity to that of a dual-substrate enzyme. The final mutant, [S15D, T17V, K109S, S292R] ttAspAT, is active toward both acidic and hydrophobic substrates. During the course of stepwise mutation, the activities toward acidic and hydrophobic substrates changed independently. The introduction of a mobile Arg292[*] residue into ttAspAT was the key step in the change to a "dual-substrate" enzyme. The substrate recognition mechanism of this thermostable "dual-substrate" enzyme was confirmed by X-ray crystallography. This work together with previous studies on various enzymes suggest that this unique "dual-substrate recognition" mechanism is a feature of not only aminotransferases but also other enzymes.

Key words: aminotransferase, dual-substrate enzyme, ping-pong bi-bi mechanism, substrate specificity, *Thermus thermophilus*.

Since the discovery that an enzyme can make a clear distinction between an L-stereo isomer and a D-isomer (*1*), enzymes have been believed to be very specific for their respective substrates. Aminotransferases, however, are unique enzymes. They are well-known vitamin B6-dependent enzymes possessing a coenzyme, pyridoxal 5′-phosphate (PLP), in their active site, and catalyze a reversible transamination reaction between an α-amino acid (α-amino acid$_1$) and an α-keto acid (α-keto acid$_2$)

$$\text{α-amino acid}_1 + \text{α-keto acid}_2 \longleftrightarrow \text{α-keto acid}_1 + \text{α-amino acid}_2 \quad \text{(Eq. 1)}$$

via the "ping-pong bi-bi" mechanism (*2–6*). The above overall-transamination reaction (Eq. 1) consists of the following two half-reactions (*4*)

$$E_{PLP} + \text{α-amino acid}_1 \longleftrightarrow E_{PMP} + \text{α-keto acid}_1 \quad \text{(Eq. 2)}$$
$$E_{PMP} + \text{α-keto acid}_2 \longleftrightarrow E_{PLP} + \text{α-amino acid}_2 \quad \text{(Eq. 3)}$$

where E_{PLP} and E_{PMP} denote the PLP and pyridoxamine 5′-phosphate (PMP) forms of the enzyme, respectively.

Our previous studies (*4*, *7*) suggested that *Escherichia coli* aspartate aminotransferase (ecAspAT) is a "dual-substrate" enzyme, and that the construction of the active site in the "dual-substrate" enzyme is achieved by the movement of a charged residue, Arg292*[3] (Fig. 6 of Ref. *7*). ecAspAT has high activity toward acidic substrates, and also low activity toward hydrophobic substrates (*4*, *7*). In the absence of substrate, the mobile Arg292* lies outside the active site (*8–11*). Upon binding a hydrophobic substrate, Arg292* remains outside the active site (*10*, *12*). However, when an acidic substrate is bound to the enzyme, the mobile Arg292* moves into the active site and forms bifurcated hydrogen bonds and a salt bridge with the ω-carboxylate of the substrate (*8–11*). The binding of an acidic substrate is accompanied by the large domain movement of the enzyme (*8–12*).

Contrary to this mesophilic ecAspAT, aspartate amino-

[1] This work was supported in part by the TARA (Tsukuba Advanced Research Alliance) Sakabe project and by Grants-in-Aid for Scientific Research (Nos. 11878118 and 11169224) from the Ministry of Education, Science, Sports and Culture of Japan, and a research grant from the Japan Society for the Promotion of Science ("Research for the Future" Program, No. JSPS-RFTF96L00506). The atomic coordinates and structure factors (code 1B5O, 1B5P, 5BJ4, 1GC3, 1GC4, and 1GCK) have been deposited in the Protein Data Bank, Research Collaboratory for Structural Bioinformatics, Rutgers University, New Brunswick, NJ (http://www.rcsb.org/).

[2] To whom correspondence should be addressed. Tel: +81-6-6850-5433, Fax: +81-6-6850-5442, E-mail: kuramitu@bio.sci.osaka-u.ac.jp

[3] The amino acid residues are numbered according to the sequence of pig cytosolic aspartate aminotransferase (*49*), and the residues belonging to the adjacent subunit are indicated by asterisks.

Abbreviations: PLP, pyridoxal 5′-phosphate; PMP, pyridoxamine 5′-phosphate; AspAT, aspartate aminotransferase; ecAspAT, *Escherichia coli* AspAT; ttAspAT, *Thermus thermophilus* HB8 AspAT; PCR, polymerase chain reaction; 2-CH_3-aspartate, 2-methyl-L-aspartate; NCS, non-crystallographic symmetry; PLP-aspartate, *N*-5′-phosphopyridoxyl-L-aspartate; PLP-tryptophan, *N*-5′-phosphopyridoxyl-L-tryptophan; PEG6K, polyethyleneglycol 6000; pdAroAT, *Paracoccus denitrificans* aromatic amino acid aminotransferase; [K109S] ttAspAT, mutant ttAspAT in which Lys109 is replaced by Ser; the other two mutant enzymes are represented in a similar manner as [K109S, S292R] ttAspAT, and [S15D, T17V, K109S, S292R] ttAspAT.

transferase (AspAT) from an extreme thermophile, *Thermus thermophilus* HB8 (ttAspAT), shows high activity only for acidic substrates, with very low activity for hydrophobic substrates (*13*). An X-ray crystallographic study of ttAspAT has revealed its structure with and without an acidic substrate analog, maleate (Fig. 1a) (*14*). This enzyme shows only 15% amino acid sequence homology with ecAspAT (*15*), while their secondary structures and active-site residues are similar (*8*, *9*, *11*, *14*). There are three distinct differences between ecAspAT and ttAspAT: (a) Although both evolved from the same enzyme through divergent evolution, the key residue that recognizes the acidic substrate in the active site is not conserved between these enzymes, that is, the residue recognizing the side-chain ω-carboxyl group of a substrate is the mobile Arg292* in ecAspAT (Fig. 1b) (*8*, *9*, *11*) and Lys109 in ttAspAT, which does not change its side-chain orientation (Fig. 1a) (*13*, *14*). (b) Upon substrate binding, ecAspAT undergoes a large movement of the domains, whereas ttAspAT does not. Only the N-terminal α-helix (Lys13–Val30) of ttAspAT approaches the bound substrate. (c) ecAspAT shows reactivity toward hydrophobic substrates, but ttAspAT shows very low reactivity (10^{-6} of the activity for the tryptophan substrate). The different properties of these two enzymes should be based on some structural differences in their active sites.

In this work, we found that mutations at four positions, S15D, T17V, K109S, and S292R, changed wild-type ttAspAT to a thermostable "dual-substrate" enzyme. Kinetic and X-ray crystallographic analyses of these mutant proteins indicated that the original AspAT from an extreme thermophile is intrinsically a "dual-substrate" enzyme.

Our data for thermophilic and mesophilic AspATs, as well as other enzymes, suggest that "dual-substrate" enzymes are distributed not only among transferases, but also among many other enzyme classes, and that these "dual-substrate" enzymes conform to a number of rules.

EXPERIMENTAL PROCEDURES

Preparation of Mutant Enzymes—The plasmid, pAMA, used for mutagenesis of the *T. thermophilus aspC* gene, was reported previously (*13*). Mutations were produced by polymerase chain reaction (PCR)–available site-directed mutagenesis, using the primers: 5′-GGAGTATACATATGCGCGGCCTTTCCCGAAGGGTCCAGGC-3′ and 5′-CTGAGCTCCAGGGCCTTAGCGTTCACCGCCACAA*(C/T)*GGC*GTC*GGGCTTCAT-3′ (letters in italics indicate sites of mutation) for the S15D and T17V mutations; 5′-GAGGAGACCATCGTCACCGTGGGGGGG*(G/A/T/C)(G/A/T/C)(G/C)*CAAGCGCTCTTCAACCTCTTCCAGG-3′ and 5′-CGACGGCCAGTGAATTCTCGAGGTCCACCTCCTTCCAGAG-3′ for the K109S mutation; and 5′-CAAGGCCATGGCCTCCGTCTCC*CGT*CAGTCGACCACGAGC-3′ and 5′-CGACGGCCAGTGAATTCTCGAGGTCCACCTCCTTCCAGAG-3′ for the S292R mutation. Nucleotide sequences of DNA were verified using a BigDye Terminator Cycle Sequencing Kit (PE Biosystems) and an ABI PRISM 377A DNA sequencer. Fragments of mutant ttAspATs were ligated into the corresponding sites of pAMA. The mutant enzymes were expressed in *E. coli* strain BL21(DE3) harboring the plasmid pLysE (Novagen). The enzymes were purified by procedures similar to those described previously (*13*). Wet cells were suspended in 30 mM sodium borate and 20 mM potassium phosphate buffer (pH 8.0) containing 10 mM 2-mercaptoethanol, 50 mM succinate, 5 mM 2-oxoglutarate, 50 μM PLP, and 0.2 mM EDTA, and then disrupted by sonication. The disrupted cells were heat-treated by incubation at 70°C for 15 min. After centrifugation at 8,000 rpm for 30 min, the supernatant was adjusted to pH 8.5. The supernatant loaded onto SuperQ-Toyopearl 650M was eluted with a linear gradient of 0–0.5 M NaCl in 10 mM sodium borate and 1 mM potassium phosphate buffer (pH 8.5) containing 5 mM 2-mercaptoethanol, 5 mM succinate, and 1 mM EDTA. The pooled active fractions loaded onto Phenyl-Toyopearl 650M were eluted with a linear gradient from 50 mM potassium phosphate buffer (pH 7.0) containing 20% saturated ammonium sulfate, 5 mM 2-mercaptoethanol, 5 mM succinate, and 1 mM EDTA to 10 mM potassium phosphate buffer (pH 7.0) containing 25% (v/v) ethylene glycol, 5 mM 2-mercaptoethanol, 5 mM succinate, and 1 mM EDTA. The pooled and concentrated active fractions were loaded onto Sephacryl S-200 equilibrated with 20 mM phosphate, 100 mM KCl, 5 mM succinate, and 1 mM DTT, at pH 7.0. The pooled active fractions were mixed and used for the following experiments.

Kinetic Analysis—The half-transamination reactions of the PLP form of the enzyme were performed using a stopped-flow spectrophotometer (Applied Photophysics, SX-17MV) as described previously (*4*), except that the wavelength was monitored at 380 nm instead of 360 nm. All reactions were conducted in 50 mM HEPES, 100 mM KCl, pH 8.0, and 25°C.

The kinetic parameters were determined using the following reaction mechanism (Eq. 4) and Eq. 5:

$$E + S \overset{K_s}{\rightleftharpoons} ES \overset{k_{cat}}{\underset{(ES^{\ddagger})}{\rightleftharpoons}} E + P \qquad \text{(Eq. 4)}$$

$$k_{app} = k_{max}[S]/(K_d + [S]) \qquad \text{(Eq. 5)},$$

where E is the enzyme, S the substrate, ES the enzyme–substrate complex, ES‡ the transition state, P the product, K_d the dissociation constant of ES to E + S, k_{max} the maximum rate constant for the conversion of ES to E + P, and k_{app} the apparent rate constant at a given substrate concentration.

For slow kinetic experiments, a HITACHI U-3000 spectrophotometer was employed. When the k_{app} value was directly proportional to the substrate concentration, Eq. 6, instead of Eq. 5, was used to determine the catalytic efficiency, k_{max}/K_d (*4*).

$$k_{app} = (k_{max}/K_d)[S] \qquad \text{(Eq. 6)}$$

The free energy difference between E + S and ES‡ ($\Delta G_T^{\ddagger}$) was calculated from Eq. 7.

$$\Delta G_T^{\ddagger} = RT\,(\ln(k_B T/h) - \ln(k_{max}/K_d)) \qquad \text{(Eq. 7)}$$

where R is the gas constant (1.98×10^{-3} kcal K^{-1} mol^{-1}), T the absolute temperature (298 K), k_B the Boltzmann constant (3.29×10^{-27} kcal K^{-1}), and h the Planck constant (1.58×10^{-37} kcal s) (*4*).

Preparation of Enzyme-Substrate Complexes for Crystallography—We first tried to prepare mutant ttAspATs complexed with 2-methyl-L-aspartate (2-CH_3-aspartate), maleate, or 2-methyl-L-tryptophan, by soaking the substrate analog with the crystal or by cocrystallization; these were not successful. Therefore, we synthesized *N*-5′-phosphopyridoxyl-L-aspartate (PLP-aspartate) and *N*-5′-phosphopyri-

doxyl-L-tryptophan (PLP-tryptophan) (*16*), and prepared an apoenzyme/cofactor-substrate analog, PLP-aspartate or PLP-tryptophan, complex.

The synthesis of PLP-aspartate or PLP-tryptophan was performed as follows: 2 mmol of PLP and L-aspartate or L-tryptophan was dissolved in H_2O, and the solution was adjusted to pH 9.3. The solution was treated with 0.1 M $NaBH_4$ for 8 h. The decolorized solution was acidified with formic acid, chromatographed on DOWEX 1-X8 anion-exchange-resin (bed volume 150 ml), and eluted with a linear gradient of 0.2–4.0 M formic acid. The second peak, which absorbed at 330 nm, was collected and freeze-dried.

To obtain the apoenzyme, the PMP form of the enzyme was treated with 50 mM K_2HPO_4 (pH 11.3) for 40 min at 25°C. The dissociated PMP from the enzyme was washed out with the same buffer using Centriprep YM-30. To this apoenzyme, PLP-aspartate or PLP-tryptophan was added to a five-fold concentration, and the mixtures were incubated for 60 min at 25°C to obtain the holoenzyme. In order to remove free PLP-aspartate or PLP-tryptophan, anion exchange chromatography was performed on a Mono Q HR 5/5 (Pharmacia Biotech) column. The peak fraction was washed with 5 mM HEPES (pH 8.0) containing 10 mM KCl, and the holoenzyme obtained was concentrated to about 0.2 mM.

Crystallization, Data Collection, and Refinement— ttAspATs without substrate analogs, [K109S, S292R] ttAspAT complexed with PLP-aspartate (the complex with PLP-tryptophan did not yield good crystals for analysis), and [S15D, T17V, K109S, S292R] ttAspAT complexed with PLP-aspartate or PLP-tryptophan were crystallized by the hanging drop vapor diffusion method. Four microliters of protein solution [0.2 mM protein in 5 mM HEPES buffer (pH 8.0) containing 10 mM KCl] was mixed with an equal volume of the precipitating buffer.

In the case of mutant enzymes without substrate, the precipitating buffers used were 300 mM ammonium phosphate, pH 4.3, for [K109S] ttAspAT, [K109S, S292R] ttAspAT, and [S15D, T17V, K109S, S292R] ttAspAT. X-ray diffraction data for these mutant enzymes were collected at 293 K on the BL6A station at the Photon Factory, KEK (Tsukuba), using an X-ray beam of wavelength 1.0 Å and a Fuji Imaging Plate with a screenless Weissenberg Camera (*17*). Summaries of the data collections are given in Table I. The data were processed and scaled using the programs DENZO and SCALEPACK (*18*). The initial structures of these mutants were determined using the coordinate of wild-type ttAspAT in the PLP form (PDB entry, 1BJW).

In the case of mutant enzymes complexed with substrate analog, the precipitating buffers used were 16% (w/w) polyethyleneglycol 6000 (PEG6K), 100 mM HEPES buffer, pH 7.5, for [K109S, S292R] ttAspAT complexed with PLP-aspartate, 18% (w/w) PEG6K, 100 mM HEPES buffer, pH 7.5, for [S15D, T17V, K109S, S292R] ttAspAT complexed with PLP-aspartate, or 24% (w/w) PEG6K, 100 mM HEPES buffer, pH 7.5, for [S15D, T17V, K109S, S292R] ttAspAT complexed with PLP-tryptophan. X-ray diffraction data for these complexes were collected at 293 K on a Rigaku R-AXIS IV imaging plate detector with graphite-monochromated CuKα X-rays produced from a Rigaku RU-200 rotating anode X-ray generator operating at 40 kV and 100 mA. The data were processed and scaled using the programs DENZO and SCALEPACK (*18*). The initial structures for the complexes were determined by molecular replacement with AMoRe (*19*), using the structure of wild-type ttAspAT in the PMP form complexed with maleate as the search model (PDB entry, 1BKG). The model was constructed from the dimeric molecule. Data between 15 and 4 Å were included for both the rotation and translation functions. A rotational search followed by a Patterson correla-

TABLE I. **Data collection and refined structural models for the mutants of ttAspAT.**

	[K109S]	[K109S, S292R]	[K109S, S292R] PLP-aspartate	[S15D, T17V, K109S, S292R]	[S15D, T17V, K109S, S292R] PLP-aspartate	[S15D, T17V, K109S, S292R] PLP-tryptophan
Diffraction data						
space group	$P2_12_12_1$	$P2_12_12_1$	$P2_12_12_1$	$P2_12_12_1$	$P2_1$	$P2_1$
lattice constants (Å)						
a	61.8	61.5	62.8	61.8	82.7	81.5
b	114.6	113.6	74.9	113.5	102.3	98.4
c	125.0	124.4	163.9	124.1	100.4	187.0
β (deg)	—	—	—	—	112.1	91.5
no. of subunits	2	2	2	2	4	8
resolution	2.2	1.8	2.5	2.0	3.3	3.3
observations	89,485	169,852	82,422	94,319	274,027	64,942
unique reflections	40,675	73,849	24,644	49,642	16,718	42,546
completeness (%)	88.5	90.6	89.5	83.0	80.3	96.0
R_{merge} (%)[a]	6.7	6.6	6.7	5.6	9.9	9.9
Refinement						
resolution limits (Å)	8.0–2.2	8.0–1.8	8.0–2.5	8.0–2.0	8.0–3.3	8.0–3.3
R_{factor} (%)[b]	17.8	19.3	20.5	18.5	21.7	20.3
R_{free} (%)[c]	23.7	23.9	28.4	21.5	27.7	28.2
Deviations						
bond length (Å)	0.007	0.010	0.014	0.008	0.010	0.011
bond angles (deg)	1.3	1.8	2.0	1.5	2.1	2.5
B-factors						
av main chains (Å²)	16.2	19.5	20.6	16.0	13.7	16.8
av side chains (Å²)	18.8	22.0	15.7	18.9	17.4	13.5
av cofactors (Å²)	9.5	15.0	24.8	14.3	9.0	13.4
av waters (Å²)	32.2	34.5	13.3	28.7	—	—

[a] $R_{merge} = \Sigma_{hkl}\Sigma_i |I_{hkl,i} - \langle I_{hkl}\rangle| / \Sigma_{hkl}\Sigma_i I_{hkl,i}$ where I represents observed intensity and $\langle I\rangle$ represents the mean intensity for multiple measurements. [b] $R_{factor} = \Sigma||F_{obs}| - |F_{calc}||/\Sigma|F_{obs}|$. [c] R_{free} is monitored with 10% of the reflection data excluded from the refinement.

tion refinement gave two distinct solutions, which resulted in translational solutions of one, two or four dimers in the asymmetric unit with an R_{factor} ($= \Sigma||F_{obs}|-|F_{calc}|| / \Sigma |F_{obs}|$) of 31.9, 31.3, or 32.9% for [K109S, S292R] ttAspAT complexed with PLP-aspartate, and [S15D, T17V, K109S, S292R] ttAspAT complexed with PLP-aspartate or PLP-tryptophan, respectively.

All structures were refined by simulated annealing and energy minimization with non-crystallographic symmetry (NCS) restraint using the program X-PLOR version 3.851 (*20–22*) and manual rebuilding using program O version 5.10.3 (*23*). The alternative refinement cycles were performed until no further improvements in structure and statistics were obtained. Since more than one subunit existed in an asymmetric unit in all cases, we used strict NCS constraints on all non-hydrogen atoms in the early stage of each refinement. These were replaced in the later stage by strong (500 kcal/Å^2) harmonic NCS restraints. Summaries of refinement are given in Table I. There were two to eight subunits in an asymmetric unit (Table I). The subunits were named subunit A to B, subunit A to D, or subunit A to H for two, four, or eight subunits, respectively. The structures of their independent subunits were very similar, except for [K109S, S292R] ttAspAT complexed with PLP-aspartate. The root-mean-square deviations between C_α of two independent subunits for unliganded [K109S] ttAspAT, [K109S, S292R] ttAspAT, and [S15D, T17V, K109S, S292R] ttAspAT were 0.28, 0.28, and 0.25 Å with maximum displacements of 2.0, 1.8, and 1.9 Å, respectively. The mean value of the root-mean-square deviations between the C_α of subunit A and other subunits for [S15D, T17V, K109S, S292R] ttAspAT complexed with PLP-aspartate and PLP-tryptophan were 0.04 and 0.15 Å, with maximum displacements of 0.49 and 1.0 Å, respectively. All side-chains with large displacements were distributed at the molecular surface.

In the case of [K109S, S292R] ttAspAT complexed with PLP-aspartate, we chose subunit B for the following discussion because the N-terminal α-helix (Lys13–Val30) in subunit B approached the active site as in wild-type ttAspAT when complexed with maleate, whereas subunit A did not.

Thermostability—The thermostability of [S15D, T17V, K109S, S292R] ttAspAT was measured at 222 nm with a heating rate of 1°C/min using a Jasco spectrophotometer, model J-720W, and a buffer component of 10 mM borate and 15 mM phosphate (pH 8.0).

RESULTS

The carboxylate of an acidic substrate is recognized by Lys109 in wild-type ttAspAT (Fig. 1a), whereas it is recognized by Arg292* in wild-type ecAspAT (Fig. 1b). In addition to these residues, Ser15 and Thr17, which interact with a side chain of the acidic substrate, were replaced as described below.

[K109S] ttAspAT Mutant—The positive charge of the rigid Lys109 in wild-type ttAspAT interacts with the negatively charged carboxylate of an acidic substrate, glutamate or aspartate (*14*). The active-site structure of the unliganded form of [K109S] ttAspAT is similar to that of the wild-type enzyme, except for the area around the replaced residues (Fig. 2a). C_β of this mutated Ser109 in [K109S]

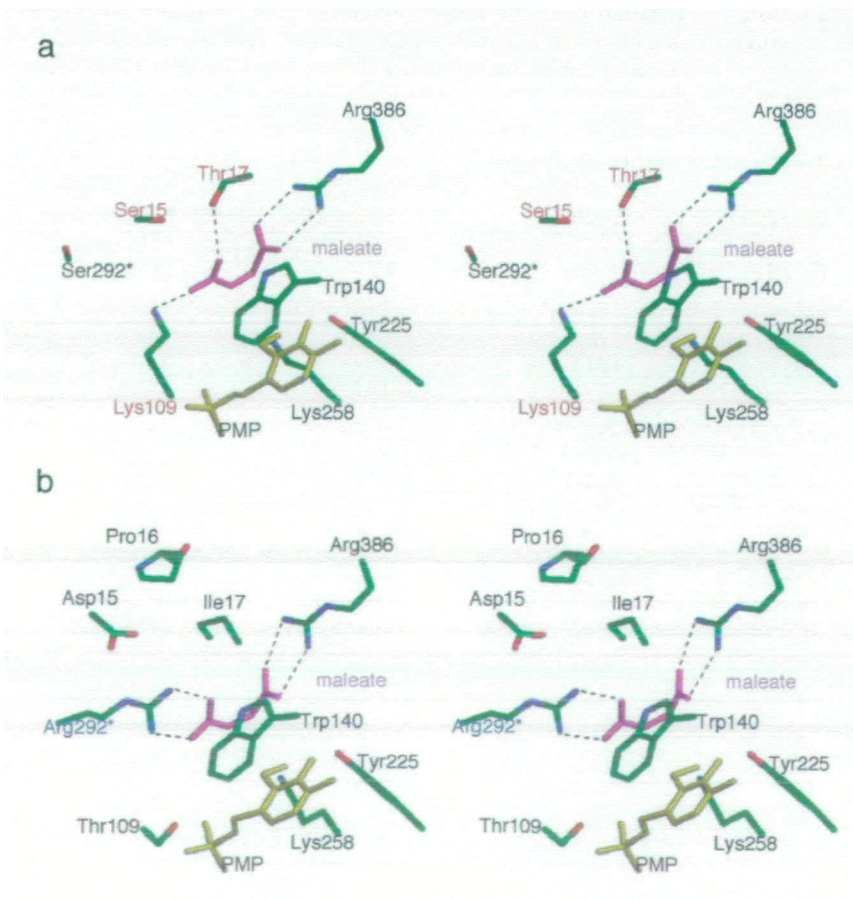

Fig. 1. **Acidic substrate recognition modes of ttAspAT and ecAspAT.** a, wild-type ttAspAT complexed with an acidic substrate analog, maleate (*14*). b, ecAspAT complexed with maleate (*9*). Maleate is colored magenta, and PMP is colored yellow. The asterisks represent residues belonging to the other subunit of the dimer.

ttAspAT is situated near (0.6 Å) that of Thr109 in ecAspAT (see Fig. 1b).

Unfortunately, we were unable to determine the k_{max} and K_d values separately, because the reaction did not show sat-

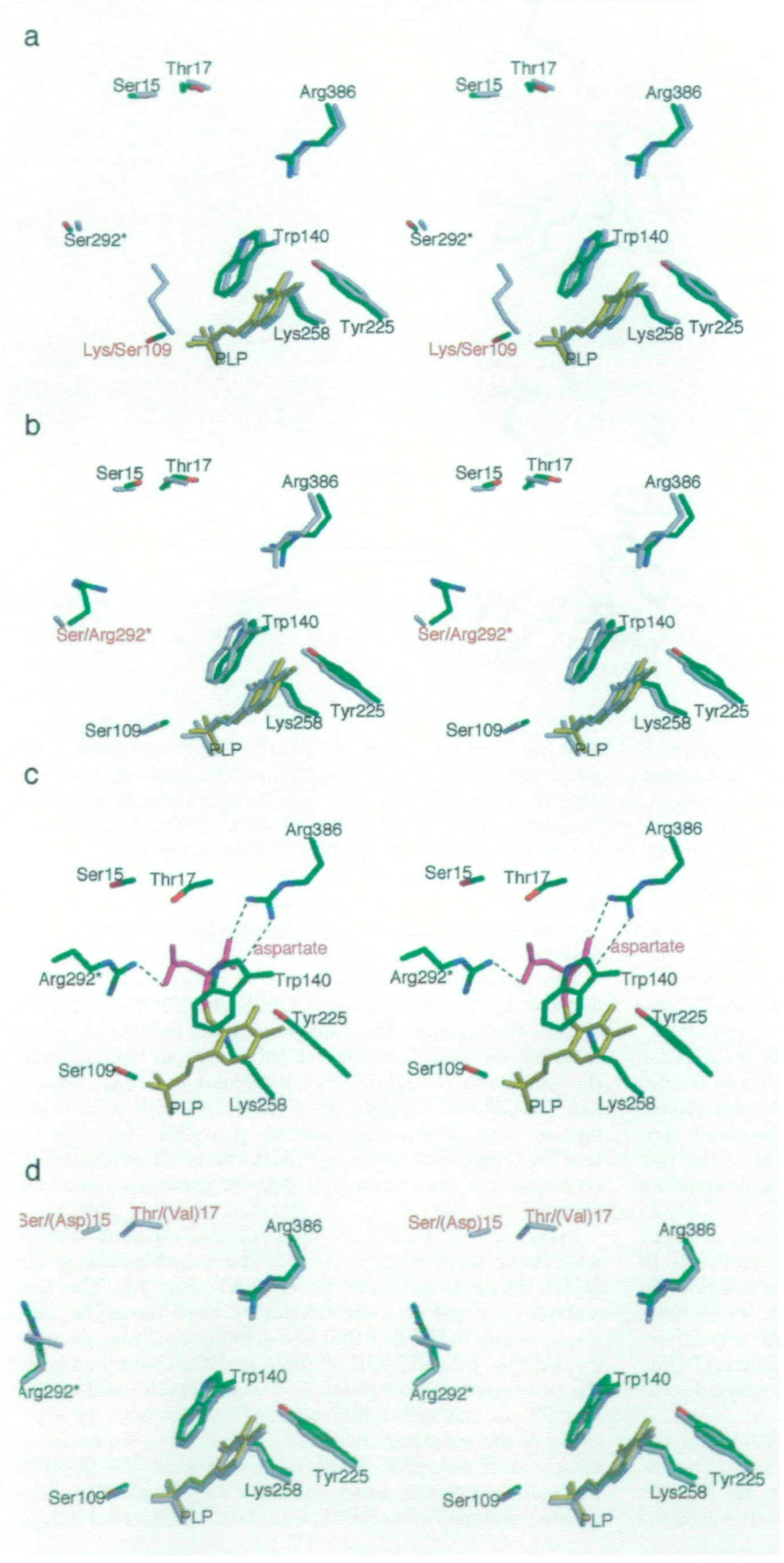

Fig. 2. **Active site structures of mutant enzymes of ttAspAT.** a, unliganded form of wild-type ttAspAT (gray) and that of [K109S] ttAspAT (PDB entry, 1B5O) (green, red, yellow, and blue). Lys/Ser109 represents Lys109 of wild-type ttAspAT replaced by Ser in [K109S] ttAspAT. b, unliganded form of [K109S] ttAspAT (gray) and that of [K109S, S292R] ttAspAT (PDB entry, 1B5P) (green, red, yellow, and blue). Ser/Arg292* represents Ser292 of [K109S] ttAspAT replaced by Arg in [K109S, S292R] ttAspAT. c, [K109S, S292R] ttAspAT complexed with PLP-aspartate (PDB entry, 1GCK). The bound aspartate moiety is colored magenta, and the PLP moiety is colored yellow. d, unliganded forms of [K109S, S292R] ttAspAT (gray) and [S15D, T17V, K109S, S292R] ttAspAT (PDB entry, 5BJ4) (green, red, yellow, and blue). Ser/(Asp)15 and Thr/(Val)17 represent Ser15 and Thr17 of [K109S, S292R] ttAspAT replaced by Asp and Val in [S15D, T17V, K109S, S292R] ttAspAT, respectively. Asp15 and Val17 in [S15D, T17V, K109S, S292R] ttAspAT are not shown because these residues are disordered in [S15D, T17V, K109S, S292R] ttAspAT. e, [S15D, T17V, K109S, S292R] ttAspAT complexed with PLP-aspartate (PDB entry, 1GC4). The bound aspartate moiety is colored magenta, and the PLP moiety is colored yellow. f, [S15D, T17V, K109S, S292R] ttAspAT with PLP-tryptophan (PDB entry, 1GC3). The bound tryptophan moiety is colored cyan and the PLP moiety is colored yellow.

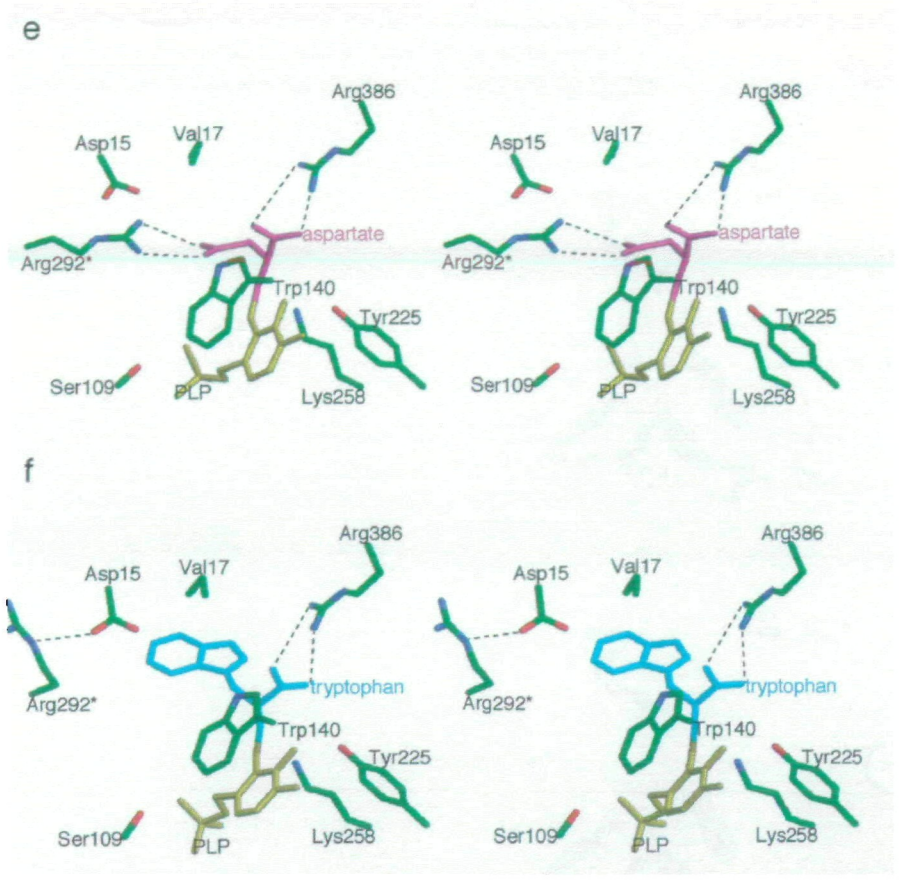

Fig. 2. e and f

uration kinetics at the substrate concentrations examined. Therefore, the values of $\Delta G_T^{\ddagger}$ (see Eq. 7) for the mutant enzyme are shown in Table II. To clarify the changes in substrate specificity among the three mutants, the values of $\Delta G_T^{\ddagger}$ toward aspartate, a representative acidic substrate, and tryptophan, a representative hydrophobic substrate, are also shown in Fig. 3.

The value of $\Delta G_T^{\ddagger}$ for an acidic substrate increased by 2.9–4.7 kcal/mol (Table II, Fig. 3), that is, the catalytic efficiency (k_{cat}/K_m) toward an acidic substrate was decreased to $\times 10^{-2}$–10^{-3}. This was due to the loss of Lys109, the key residue for the recognition of acidic substrates.

This mutation, however, lowered the value of $\Delta G_T^{\ddagger}$ for hydrophobic substrates by 2.1–6.1 kcal/mol (Table II, Fig. 3), and increased the catalytic efficiency for hydrophobic substrates. This was due to a decrease in the steric hindrance of residue 109 in the rigid region, and to the fact that ttAspAT potentially possesses the substrate-binding pocket for a hydrophobic substrate.

[K109S, S292R] ttAspAT Mutant—The mobile Arg292*, which recognizes the ω-carboxyl group of the substrate in ecAspAT (*8–11*), was introduced into [K109S] ttAspAT. In the crystal structure of the unliganded form of [K109S, S292R] ttAspAT, the newly introduced Arg292* was directed toward the surface of the molecule, as in ecAspAT (Fig. 2b). The conformation of the other part of the molecule was similar to that of [K109S] ttAspAT.

Contrary to expectation, a mutation of S292R did not increase the reactivity of [K109S] ttAspAT toward acidic substrates (Table II, Fig. 3). The property of [K109S, S292R] ttAspAT complexed with PLP-aspartate suggested that the N-terminal α-helix (Lys13–Val30) approaches the active site as wild-type ttAspAT, and that the side-chain of Arg292* is directed into the active site of subunit B with a closed form (see "EXPERIMENTAL PROCEDURES"). However, the mobile Arg292* of [K109S, S292R] ttAspAT could not form a bifurcated salt bridge with the side-chain of the substrate (Fig. 2c). This would explain the lower activity of [K109S, S292R] ttAspAT toward acidic substrates compared with that of ecAspAT.

The activity toward hydrophobic substrates was not affected by the mutation of S292R in [K109S] ttAspAT (Table II, Fig. 3). This suggests that [K109S, S292R] ttAspAT can bind hydrophobic substrates without moving the side-chain of Arg292*. The molecular dynamic simulation of [K109S, S292R] ttAspAT complexed with tryptophan suggests that the direction of Arg292* is similar to that in unliganded form, and that the binding pocket for tryptophan is not identical to that for aspartate (data not shown).

[S15D, T17V, K109S, S292R] ttAspAT Mutant—Ser15 and Thr17 interact with the side-chain carboxylate of an acidic substrate in wild-type ttAspAT (Fig. 1a). The low activity of [K109S, S292R] ttAspAT toward the acidic substrate is due to the fact that the polar interactions present in wild-type ttAspAT (OH of Ser15 and Thr17 interact with the side-chain carboxylate (*14*)) still remain and, thus, Arg292* can not form a bifurcated salt bridge with the side-chain of the substrate. According to the three-dimensional structure of ecAspAT, Ser15 is located near the position equivalent to Asp15, which interacts with Arg292* in unliganded ecAspAT (*8*). Ser15 was, then, replaced by Asp.

Since the Val or Ile residue at position 17 is conserved among mesophilic AspATs, Thr17 is replaced by Val, which has a volume similar to that of Thr (*14*). The resulting mutant enzyme, [S15D, T17V, K109S, S292R] ttAspAT, has an active-site structure of the unliganded form similar to that of [K109S, S292R] ttAspAT (Fig. 2d). However, the N-terminal α-helix region (Asp15–Gly30) of this tetra mutant is very flexible and lacks any convincing electron density on the Fourier map (data not shown).

This mutant, [S15D, T17V, K109S, S292R] ttAspAT, shows higher activity than [K109S, S292R] ttAspAT toward the acidic substrate, aspartate (a $\Delta G_T^{\ddagger}$ value lower by 1.4 kcal/mol), and toward most hydrophobic substrates ($\Delta G_T^{\ddagger}$ values lower by 0.7–3.8 kcal/mol), whereas its activity is similar to that of [K109S, S292R] ttAspAT for the acidic substrate, glutamate (Table II, Fig. 3). It is curious that the activity toward an acidic substrate is increased by the introduction of a negatively charged (acidic) residue. Some specific interactions may be formed in the active site of [S15D, T17V, K109S, S292R] ttAspAT upon binding to an acidic substrate. [S15D, T17V, K109S, S292R] ttAspAT also

TABLE II. **Kinetic parameters [$\Delta G_T^{\ddagger}$ (kcal/mol)] of the half reaction of wild type and mutant ttAspAT and ecAspAT for natural substrates.**

Substrate	ttAspAT				ecAspAT[b]
	Wild type[a] $\Delta G_T^{\ddagger}$	[K109S] $\Delta G_T^{\ddagger}$	[K109S, S292R] $\Delta G_T^{\ddagger}$	[S15D, T17V, K109S, S292R] $\Delta G_T^{\ddagger}$	$\Delta G_T^{\ddagger}$
Asp	9.9	14.6[a,c]	17.6	16.2	10.4
Glu	12.6	15.5[a]	18.8	19.0	11.5
Ala	18.9	16.3[a]	17.2	16.5	17.9
Ser	19.3	16.5	18.1	17.1	19.3
Asn	18.6	14.9	17.6	16.2	17.3
Gln	19.5	15.5	17.3	15.9	17.6
His	20.3	14.2[c]	16.6	14.8[c]	15.9
Met	17.1	15.0	16.9	14.9	15.6
Thr	n.d.[d]	20.2	21.7	19.2	20.3
Val	22.4	19.2	21.3	19.3	21.1
Leu	19.4	16.4	18.1	15.6	17.5
Ile	21.1	19.0	21.6	19.5	n.d.[d]
Lys	19.9	17.8	18.1	16.8	20.1
Arg	20.6	17.3	17.8	16.5	20.3
Phe	20.5	17.0	17.8	15.6	14.3
Tyr	n.d.[d]	16.3	18.4	14.6[c]	13.6
Trp	20.2	14.7[c]	14.1[c]	12.0[c]	13.5

Measurement conditions: 50 mM HEPES, 100 mM KCl, 0.01 mM EDTA, pH 8.0, at 25°C. [a]Data from Ref. *13*. [b]Data from Ref. *4*. [c]Data measured with a stopped-flow spectrophotometer. [d]No reaction was detected at the substrate concentrations examined. $\Delta G_T^{\ddagger}$ was calculated from the following equation (*4*): $\Delta G_T^{\ddagger} = RT\,[\ln(k_B T/h) - \ln(k_{mar}/K_d)]$.

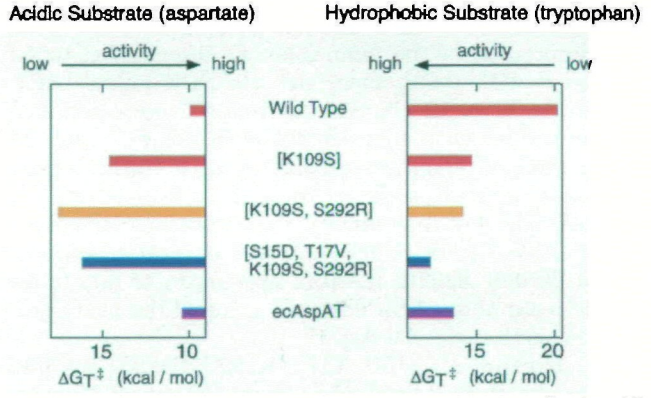

Fig. 3. **Free energy changes for mutant enzymes of ttAspAT toward aspartate and tryptophan.** Changes of activity toward an acidic substrate, aspartate, and a hydrophobic substrate, tryptophan, among mutant enzymes of ttAspAT are shown.

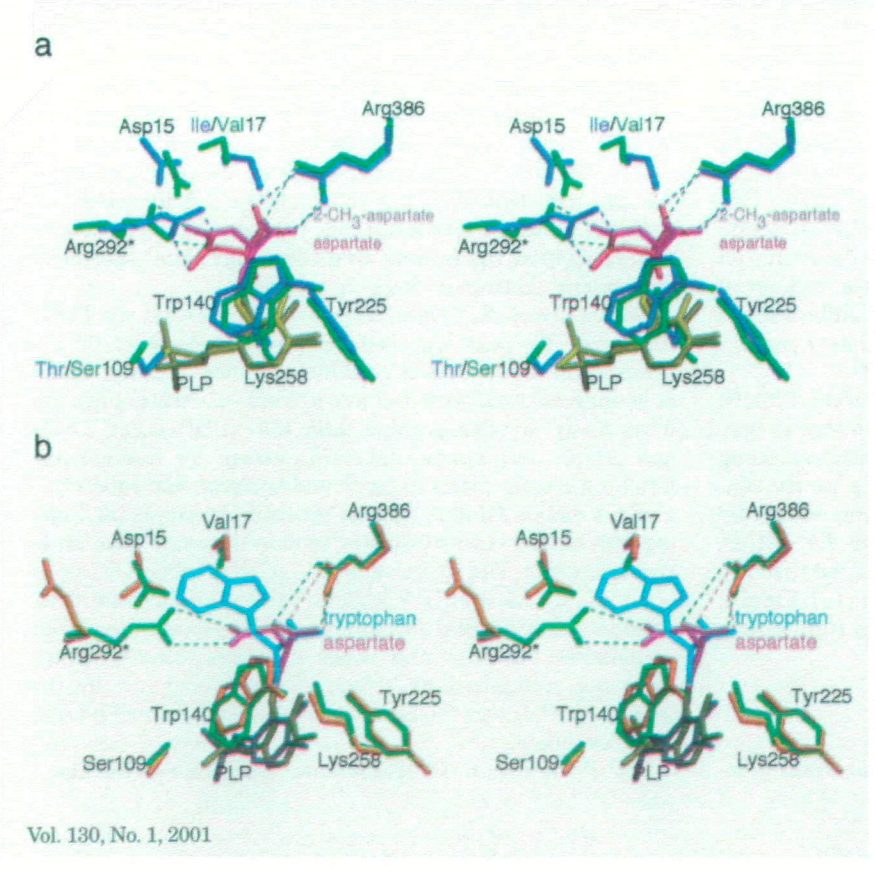

Fig. 4. **Superimposed active-site structures of [S15D, T17V, K109S, S292R] ttAspAT with substrate analogs.** a, [S15D, T17V, K109S, S292R] ttAspAT (green) with PLP-aspartate (yellow shows the PLP moiety and magenta shows the aspartate moiety in [S15D, T17V, K109S, S292R] ttAspAT), and ecAspAT (light blue) with 2-CH_3-aspartate (dark yellow shows PLP and pink shows 2-CH_3-aspartate in ecAspAT) (*8*). b, [S15D, T17V, K109S, S292R] ttAspAT (green) complexed with PLP-aspartate (gold shows the PLP moiety and magenta shows the aspartate moiety in the complex with PLP-aspartate) and the same mutant (orange) of PLP-tryptophan form (gray shows the PLP moiety and cyan shows the tryptophan moiety in the complex with PLP-tryptophan).

shows high activity toward hydrophobic substrates. [S15D, T17V, K109S, S292R] ttAspAT can thus bind both acidic and hydrophobic substrates. We then determined the three-dimensional structures of the PLP-aspartate and PLP-tryptophan forms of [S15D, T17V, K109S, S292R] ttAspAT to compare them with those of [K109S, S292R] ttAspAT.

The structure of [S15D, T17V, K109S, S292R] ttAspAT complexed with PLP-aspartate shows that the N-terminal α-helix, disordered in the unliganded form, is fixed and situated at almost the same position as in the liganded form of wild-type ttAspAT (data not shown). The newly introduced Arg292*, which is directed toward the surface of the molecule in the absence of a substrate analog, orients its side-chain into the active site to form bifurcated hydrogen bonds and a salt bridge with the ω-carboxyl group of the substrate (Fig. 2e). Asp15 interacts electrostatically with the mobile Arg292*, but not [K109S, S292R] ttAspAT. Val17 does not interact with ω-carboxyl group of the substrate. Superimposition of the main-chain C_α atoms of ecAspAT complexed with 2-CH_3-aspartate (*10*; PDB entry, 1ART) and [S15D, T17V, K109S, S292R] ttAspAT complexed with PLP-aspartate shows that Arg292* of [S15D, T17V, K109S, S292R] ttAspAT and the ω-carboxyl group of the acidic substrate are situated at almost the same positions those in ecAspAT (Fig. 4a). In summary, the enhanced reactivity of [S15D, T17V, K109S, S292R] ttAspAT in comparison with that of [K109S, S292R] ttAspAT appears to be due to the specific recognition of the carboxyl group of the acidic substrate, as is the case of ecAspAT.

The structure of [S15D, T17V, K109S, S292R] ttAspAT complexed with PLP-tryptophan suggests that the N-terminal α-helix, disordered in the unliganded form, is ordered as that in the PLP-aspartate form (data not shown). The indole moiety of PLP-tryptophan binds to a potential hydrophobic pocket of [S15D, T17V, K109S, S292R] ttAspAT. The newly introduced Arg292* does not change its side-chain orientation and interacts with Asp15, unlike the case for an acidic substrate (Fig. 2f). Due to this neutralization of positively charged Arg292* by Asp15, the reactivity of [S15D, T17V, K109S, S292R] ttAspAT for hydrophobic substrates is higher than that of [K109S, S292R] ttAspAT. In order to compare the binding modes of acidic and hydrophobic substrates, the active-site residues of [S15D, T17V, K109S, S292R] ttAspAT complexed with PLP-aspartate and PLP-tryptophan were superimposed by centering on their C_α atoms (Fig. 4b). The side-chain orientations of these two substrates are similar, but slightly different (the angle between C_α-C_γ of the bound aspartate moiety and C_α-$C_{\eta 2}$ of the bound tryptophan moiety is about 30°).

These results suggest that [S15D, T17V, K109S, S292R] ttAspAT binds both acidic and hydrophobic substrates specifically by changing the properties of its substrate binding pocket. The mutant enzyme is found to be a newly constructed thermostable "dual-substrate" enzyme, since the midpoint of the thermal denaturation curve for [S15D, T17V, K109S, S292R] ttAspAT is about 88°C, similar to the thermal stability of wild-type ttAspAT (90°C) (*15*). Finally, it is suggested that "dual-substrate" enzymes represent a general strategy for aminotransferases.

DISCUSSION

Construction of a Thermophilic "Dual-Substrate" Enzyme—It has been believed that enzymes show very strict substrate specificities toward respective substrates (*1*) ("one enzyme–one substrate" enzyme). In this study, we changed the active-site residues of ttAspAT and constructed the mutants [K109S] ttAspAT, [K109S, S292R] ttAspAT, and [S15D, T17V, K109S, S292R] ttAspAT. We then performed structural (Figs. 1, 2, and 4) and kinetic (Table II, Fig. 3) analyses of these mutant enzymes. Although the initial wild-type ttAspAT, which shows high activity toward the acidic substrate, seemed to be a "one enzyme–one substrate" enzyme, the properties of [K109S] ttAspAT showed that ttAspAT has the potential to bind hydrophobic substrates. This is because Lys109 is situated in a rigid region of the enzyme molecule (*13*, *14*) and creates steric hindrance toward the hydrophobic substrate. The final mutant, [S15D, T17V, K109S, S292R] ttAspAT, was shown to be able to bind both acidic and hydrophobic substrates in a specific manner using the mobile Arg292* and its potential hydrophobic binding pocket. These results suggest that the enzyme with a rigid Lys109 located near the catalytic group (*13*, *14*) is a "one enzyme–one substrate" enzyme, whereas the enzyme with a mobile Arg292* located far from the catalytic group (*7*) is a "dual-substrate" enzyme. In summary, the mutant enzyme obtained was a thermostable "dual-substrate" enzyme, and thus aminotransferases are unique "dual-substrate" enzymes.

Generality of the "Dual-Substrate" Property for Aminotransferases—The unique "dual-substrate" property of aminotransferases is intuitively reasonable, since these enzymes need to transfer an amino group between two different kinds of substrates. Previous studies of many aminotransferases have been based only on kinetic analyses (*24–26*), whereas *Paracoccus denitrificans* aromatic amino acid aminotransferase (pdAroAT) was reported to be a "dual-substrate" enzyme on the basis of both kinetics (*27*) and X-ray crystallographic data (*28*) (PDB entry, 1AY5 and 1AY8). Okamoto *et al.* (*28*) have suggested that both substrates bind to the same position in the active site. The binding site for acidic and hydrophobic substrates with ecAspAT (*12*) and its hexamutant (*10*) is identical to that of pdAroAT. In all three enzymes, the hinge atom, C_α, of the mobile Arg292* is located distant from the ε-NH_2 group of the catalytic Lys258 (13.5, 13.0, and 13.7 Å for pdAroAT, ecAspAT, and its hexamutant, respectively). The above results support the concept that "dual-substrate" specificity is a general feature of aminotransferases.

Generality of the "Dual-Substrate" Mechanism for Other Enzymes—We next searched for other "dual-substrate" enzymes, and found that a cysteine protease, cruzain, is the only enzyme considered to have a "dual-substrate" property from X-ray crystallographic data (*29*) (PDB entry, 1AIM and 2AIM) and kinetic data (*30*), except for aminotransferases. Cruzain binds to basic and hydrophobic substrates using a mobile Glu205 and its potential hydrophobic binding pocket, and both substrates bind to the same position in the active site. The hinge atom, C_α, of the mobile Glu205 is about 12.5, 13.5, and 16.0 Å distant from the three catalytic residues, Cys25, His159, and Asn175, respectively. Other transferases (*31–37*) and other enzymes (*38–48*), which were not recognized as "dual-substrate" enzymes by the original authors on the basis of kinetic studies, may be possible candidates.

The Principle of "Dual-Substrate" Enzymes—The above

results indicate that the mobile and charged key residue in a "dual-substrate" enzyme is located slightly apart from the catalytic residue, which is usually situated in a very rigid part of the molecule. There are many enzymes, such as wild-type ttAspAT, that show strict substrate specificity. Some enzymes can show substantial changes in their substrate specificity as a result of certain amino acid mutations. By applying this strategy to ttAspAT, we have been able to create a thermophilic "dual-substrate" enzyme, and also formulate a general mechanism for "dual-substrate" enzymes as a whole.

We would like to thank Professor Emeritus N. Sakabe (National Laboratory for High Energy Physics), and Drs. N. Igarashi and M. Suzuki (High Energy Accelerator Research Organization) for their help in data collection through synchrotron radiation. We thank Drs. J. Ishijima and M. Sugahara of RIKEN Harima Institute/SPring-8, and Dr. N. Nakagawa of Osaka University for helpful discussions.

REFERENCES

1. Fischer, E. (1894) Einfluss der Configuration auf die Wirkung Derenzyme. *Ber. Dt. Chem. Ges.* **27**, 2895–2993
2. Velick, S.F. and Vavra, J. (1962) A kinetic and equilibrium analysis of the glutamic oxaloacetate transaminase mechanism. *J. Biol. Chem.* **237**, 2109–2122
3. Kiick, D.M. and Cook, P.F. (1983) pH studies toward the elucidation of the auxiliary catalist for pig heart aspartate aminotransferase. *Biochemistry* **22**, 375–382
4. Kuramitsu, S., Hiromi, K., Hayashi, H., Morino, Y., and Kagamiyama, H. (1990) Pre-steady-state kinetics of *Escherichia coli* aspartate aminotransferase catalyzed reactions and thermodynamic aspects of its substrate specificity. *Biochemistry* **29**, 5469–5476
5. Kirsch, J.F., Eichele, G., Ford, G.C., Vincent, M.G., Jansonius, J.N., Gehring, H., and Christen, P. (1984) Mechanism of action of aspartate aminotransferase proposed on the basis of its spatial structure. *J. Mol. Biol.* **174**, 497–525
6. Jenkins, W.T. and Fonda, M.L. (1985) *Transaminases* (Christen, P. and Metzler, D.E., eds.) pp. 215–234, John Wiley & Sons, New York
7. Kawaguchi, S., Nobe, Y., Yasuoka, J., Wakamiya, T., Kusumoto, S., and Kuramitsu, S. (1997) Enzyme flexibility: a new concept in recognition of hydrophobic substrates. *J. Biochem.* **122**, 55–63
8. Okamoto, A., Higuchi, T., Hirotsu, K., Kuramitsu, S., and Kagamiyama, H. (1994) X-ray crystallographic study of pyridoxal 5'-phosphate-type aspartate aminotransferases from *Escherichia coli* in open and closed form. *J. Biochem.* **116**, 95–107
9. Miyahara, I., Hirotsu, K., Hayashi, H., and Kagamiyama, H. (1994) X-ray crystallographic study of pyridoxamine 5'-phosphate-type aspartate aminotransferases from *Escherichia coli* in three forms. *J. Biochem.* **116**, 1001–1012
10. Malashkelvich, V.N., Onuffer, J.J., Kirsch, J.F., and Jansonius, J.N. (1995) Alternating arginine-modulated substrate specificity in an engineered tyrosine aminotransferase. *Nat. Struct. Biol.* **2**, 548–553
11. Jäger, J., Moser, M., Sauder, U., and Jansonius, J.N. (1994) Crystal structures of *Escherichia coli* aspartate aminotransferase in two conformations. Comparison of an unliganded open and two liganded closed forms. *J. Mol. Biol.* **239**, 285–305
12. Ishijima, J., Nakai, T., Kawaguchi, S., Hirotsu, K., and Kuramitsu, S. (2000) Free energy requirement for domain movement of an enzyme. *J. Biol. Chem.* **275**, 18939–18945
13. Nobe, Y., Kawaguchi, S., Ura, H., Nakai, T., Hirotsu, K., Kato, R., and Kuramitsu, S. (1998) The novel substrate recognition mechanism utilized by aspartate aminotransferase of the extreme thermophile *Thermus thermophilus* HB8. *J. Biol. Chem.* **273**, 29554–29564
14. Nakai, T., Okada, K., Akutsu, S., Miyahara, I., Kawaguchi, S., Kato, R., Kuramitsu, S., and Hirotsu, K. (1999) Structure of *Thermus thermophilus* HB8 aspartate aminotransferase and its complex with maleate. *Biochemistry* **38**, 2413–2424
15. Okamoto, A., Kato, R., Masui, R., Yamagishi, A., Oshima, T., and Kuramitsu, S. (1996) An aspartate aminotransferase from an extremely thermophilic bacterium, *Thermus thermophilus* HB8. *J. Biochem.* **119**, 135–144
16. Severin, E.S., Gulyaev, N.N., Khurs, E.N., and Khomutov, R.M. (1969) The synthesis and properties of phosphopyridoxyl amino acids. *Biochem. Biochem. Biophys. Res. Commun.* **35**, 318–323
17. Sakabe, N. (1991) X-ray diffraction data collection system for modern protein crystallography with weissenberg camera and an imaging plate using synchrotron radiation. *Nucl. Instrum. Methods Phys. Res. A* **303**, 448–463
18. Otwinowski, Z. (1993) *Data Collection and Processing, Proceeding of the CCP4 Study Weekend*, pp. 56–62, Daresbury Laboratory, Warrington, England
19. Navaza, J. (1994) AMoRe: an automated package for molecular replacement. *Acta Crystallogr. A* **50**, 157–163
20. Brünger, A.T. (1991) Simulated annealing in crystallography. *Annu. Rev. Phys. Chem.* **42**, 197–223
21. Brünger, A.T. (1993) *X-PLOR Version 3.1: A System for X-Ray Crystallography and NMR*, Yale University Press, New Haven, CT
22. Brünger, A.T., Kuriyan, J., and Karplus, M. (1987) Crystallographic R factor refinement by molecular dynamics. *Science* **235**, 458–460
23. Jones, T.A., Zou, J.-Y., Cowan, S.W., and Kjeldgaard, M. (1991) Improved methods for building protein models in electron density maps and the location of errors in these models. *Acta Crystallogr. A* **47**, 110–119
24. Kirsch, J.F. and Onuffer, J.J. (1994) *Biochemistry of Vitamin B6 and PQQ* (Bossa, F. *et al.*, eds.) pp. 37–41, Birkhauser Verlag, Basel
25. Hayashi, H., Inoue, K., Nagata, T., Kuramitsu, S., and Kagamiyama, H. (1993) *Escherichia coli* aromatic amino acid aminotransferase: characterization and comparison with aspartate aminotransferase. *Biochemistry* **32**, 12229–12239
26. Son, D., Jo, J., and Sugiyama, T. (1991) Purification and characterization of alanine aminotransferase from *Panicum miliaceum* leaves. *Arch. Biochem. Biophys.* **289**, 262–266
27. Oue, S., Okamoto, A., Nakai, Y., Nakahira, M., Shibatani, T., Hayashi, H., and Kagamiyama, H. (1997) *Paracoccus denitrificans* aromatic amino acid aminotransferase: a model enzyme for study of dual substrate recognition. *J. Biochem.* **121**, 161–171
28. Okamoto, A., Nakai, Y., Hayashi, H., Hirotsu, K., and Kagamiyama, H. (1998) *Paracoccus denitrificans* aromatic amino acid aminotransferase: a model enzyme for study of dual substrate recognition. *J. Mol. Biol.* **280**, 443–461
29. Gillmor, S.A., Craik, C.S., and Fletterick, R.J. (1997) Structural determinants of specificity in the cystein protease cruzain. *Protein Sci.* **6**, 1603–1611
30. Serveau, C., Lalmanach, G., Juliano, M.A., Scharfstein, J., Juliano, L., and Gauthier, F. (1996) Investigation of the substrate specificity of cruzipain, the major cysteine protease of *Trypanosoma cruzi*, through the use of cystatin-derived substrate and inhibitors. *Biochem. J.* **313**, 951–956
31. Lu, T., Li, Q., Katoh, A., Hernandez, J., Duffin, K., Jackson-Machelski, E., Knoll, L.J., Gokel, G.W., and Gordon, J.I. (1994) The substrate specificity of *Saccharomyces cerevisiae* myristoyl-CoA: protein N-myristoyltransferase. Polar probes of the enzyme's myristoyl-CoA recognition site. *J. Biol. Chem.* **269**, 5346–5357
32. Antonenkov, V.D., Van Veldhoven, P.V., Waelkens, E., and Mannaerts, G.P. (1997) Substrate specificities of 3-oxoacyl-CoA thiolase A and sterol carrier protein 2/3-oxoacyl-CoA thiolase purified from normal rat liver peroxisomes. Sterol carrier protein 2/3-oxyoacetyl-CoA thiolase is involved in the metabolism of 2-methyl-branched fatty acids and bile acid intermediates. *J. Biol. Chem.* **272**, 26023–26031

33. Moores, S.L., Schaber, M.D., Mosser, S.D., Rands, E., O'Hara, M.B., Garsky, V.M., Marshall, M.S., Pompliano, D.L., and Gibbs, J.B. (1991) Sequence dependence of protein isoprenylation. *J. Biol. Chem.* **266**, 14603–14610
34. Buckel, W., Dorn, U., and Semmler, R. (1981) Glutaconate CoA-transferase from *Acidaminococcus fermentans*. *Eur. J. Biochem.* **118**, 315–321
35. Maxwell, C.A., Edwards, R., and Dixon, R.A. (1992) Identification, purification, and characterization of *S*-adenosyl-L-methionine: isoliquiritigenin 2′-*o*-methyltransferase from alfalfa (*Medicago sative* L.). *Arch. Biochem. Biophys.* **293**, 158–166
36. Foote, J., Lauritzen, A.M., and Lipscomb, W.N. (1985) Substrate specificity of aspartate transcarbamylase. Interaction of the enzyme with analogs of aspartate and succinate. *J. Biol. Chem.* **260**, 9624–9629
37. Lo Bello, M., Oakley, A.J., Battistoni, A., Mazzetti, A.P., Nuccetelli, M., Mazzarese, G., Rossjohn, J., Parker, M.W., and Ricci, G. (1997) Multifunctional role of Tyr 108 in the catalytic mechanism of human glutathione transferase P1-1. Crystallographic and kinetic studies on the Y108F mutant enzyme. *Biochemistry* **36**, 6207–6217
38. Waksman, G., Kominos, D., Robertson, S.C., Pant, N., Baltimore, D., Birge, R.B., Cowburn, D., Hanafusa, H., Mayer, B.J., Overduin, M., Resh, M.D., Rios, C.B., Silverman, L., and Kuriyan, J. (1992) Crystal structure of the phosphotyrosine recognition domain SH2 of v-src complexed with tyrosine-phosphorylated peptides. *Nature* **358**, 646–653
39. Sohling, B. and Gottschalk, G. (1993) Purification and characterization of a coenzyme-A-dependent succinate-semialdehyde dehydrogenase from *Clostridium klutveri*. *Eur. J. Biochem.* **212**, 121–127
40. Mihara, H., Kurihara, T., Yoshimura, T., Soda, K., and Esaki, N. (1997) Cysteine sulfinate desulfinase, a NIFS-like protein of *Escherichia coli* with selenocysteine lyase and cysteine desulfurase activities. Gene cloning, purification, and characterization of a novel pyridoxal enzyme. *J. Biol. Chem.* **272**, 22417–22424
41. Wise, M.L., Rossi, J., and Gerwick, W.H. (1997) Characterization of the substrate binding site of polyenoic fatty acid isomerase, a novel enzyme from the marine alga *Ptilota filicina*. *Biochemistry* **36**, 2985–2992
42. Westphal, V., Spetzler, J.C., Meldal, M., Christensen, U., and Winther, J.R. (1998) Kinetic analysis of the mechanism and specificity of protein-disulfide isomerase using fluorescence-quenched peptides. *J. Biol. Chem.* **273**, 24992–24999
43. Rella, R., Raia, C.A., Pensa, M., Pisani, F.M., Gambacorta, A., De-Rosa, M., and Rossi, M. (1987) A novel archaebacterial NAD^+-dependent alcohol dehydrogenase. Purification and properties. *Eur. J. Biochem.* **167**, 475–479
44. Van Etten, R.L. and Waymack, P.P. (1991) Substrate specificity and pH dependence of homogeneous wheat germ acid phosphatase. *Arch. Biochem. Biophys.* **288**, 634–645
45. Sundraraju, B., Antson, A.A., Phillips, R.S., Demidkina, T.V., Barbolina, M.V., Gollnick, P., Dodson, G.G., and Wilson, K.S. (1997) The crystal structure of *Citrobacter freundii* tyrosine phenol-lyase complexed with 3-(4′-hydroxyphenyl)-propionic acid, together with site-directed mutagenesis and kinetic analysis, demonstrates that arginine 381 is required for substrate specificity. *Biochemistry* **36**, 6502–6510
46. Prucha, M., Peterseim, A., Timmis, N., and Pieper, D.H. (1996) Muconolactone isomerase of the 3-oxoadipate pathway catalyzes dechlorination of 5-chloro-substituted muconolactones. *Eur. J. Biochem.* **237**, 350–356
47. Glasemacher, J., Bock, A.-K., Schmid, R., and Schonheit, P. (1997) Purification and properties of acetyl-CoA synthetase (ADP-forming), an archaeal enzyme of acetate formation and ATP synthesis, from the hyperthermophiles *Pyrococcus furiosus*. *Eur. J. Biochem.* **244**, 561–567
48. Habeck, L.L., Mendelsohn, L.G., Shin, C., Taylor, E.C., Colman, P.L., Gossett, L.S., Leitner, T.A., Schultz, R.M., and Andis, S.L. (1995) Substrate specificity of mammalian folylpolyglutamate synthetase for 5,10-dideazatetrahydrofolate analogs. *Mol. Pharmacol.* **48**, 326–333
49. Mehta, P.K., Hale, T.I., and Christen, P. (1989) Aminotransferases: demonstration of homology and division into evolutionary subgroups. *Eur. J. Biochem.* **186**, 249–253